Available online at www.sciencedirect.com
SCIENCE DIRECT®
International Journal of Heat and Mass Transfer 49 (2006) 3167–3179
International Journal of HEAT and MASS TRANSFER
www.elsevier.com/locate/ijhmt

Onset of oscillatory thermocapillary convection in acetone liquid bridges: The effect of evaporation

S. Simic-Stefani [a], M. Kawaji [a], S. Yoda [b,*]

[a] Department of Chemical Engineering and Applied Chemistry, University of Toronto, 200 College Street, Toronto, Ont., Canada M5S 3E5
[b] Institute of Space and Astronautical Sciences, Space Biology and Microgravity Sciences Department, Japan Aerospace Exploration Agency, Tsukuba-shi, Ibaraki-ken 305-8505, Japan

Received 10 November 2004
Available online 17 April 2006

Abstract

Experiments have been carried out for half-zones of acetone ($Pr = 4.3$) to investigate the effects of evaporative cooling on the flow structures and temperature fields during transition from steady to oscillatory convection. The unstable flow phenomena have been measured using a variety of diagnostic techniques to determine the effects of evaporative cooling on Marangoni convection in liquid bridges of intermediate Prandtl number. The results show that Marangoni convection in acetone liquid bridges with and without strong evaporation becomes unstable due to the same mechanism but the evaporation has a strong stabilizing effect on the onset of oscillatory Marangoni convection.
© 2006 Elsevier Ltd. All rights reserved.

Keywords: Marangoni convection; Half-zones; Evaporation effects; Oscillatory convection; Floating zone; Stability

1. Introduction

Thermocapillary or Marangoni convection in a cylindrical liquid bridge formed between heated and cooled circular disks is important for understanding the transport processes involved in the floating zone crystal growth. The quality of crystals grown may be adversely affected when Marangoni convection undergoes transition from a steady to oscillatory state. The resulting temperature and velocity oscillations in the melt could cause striations to appear in the crystal.

Marangoni convection experiments in half-floating zones (half-zones) have been extensively conducted in the past under normal gravity on the ground and under microgravity aboard the Space Shuttle as well as on various sounding rockets. It has been experimentally observed that above a certain critical temperature difference, ΔT_c, or a suitably defined critical Marangoni number, Ma_c, the Marangoni convection in a half zone of high Prandtl number fluids undergoes a transition from steady to oscillatory convection (see [1–4]; among others). For lower values of the Marangoni number, a steady flow is observed with a single, axisymmetric toroidal vortex. When the critical Marangoni number is exceeded, the flow and liquid temperature would become oscillatory. A comprehensive review of experiments on thermocapillary instabilities was recently presented by Schatz and Neitzel [5].

The past experiments have been conducted by mostly employing high Prandtl number fluids ($Pr > 10$). The results have indicated that the critical Marangoni number varies with the Prandtl number, disk diameter, liquid volume, and aspect ratio ($\Gamma =$ height/radius) of the liquid bridge. On the other hand, numerical analyses of high Prandtl number experiments encounter considerable difficulties due to a thin thermal boundary layer and its implications for finer grid resolution.

The numerical difficulty associated with the thin thermal boundary layer is alleviated when Marangoni convection at intermediate Prandtl numbers, up to about 10, is examined.

* Corresponding author. Tel.: +81 3 3788 0728; fax: +81 298 50 2233.
E-mail address: yoda.shinichi@jaxa.jp (S. Yoda).

0017-9310/$ - see front matter © 2006 Elsevier Ltd. All rights reserved.
doi:10.1016/j.ijheatmasstransfer.2006.01.042

Nomenclature

D	liquid bridge diameter [m]
H	liquid bridge height [m]
Ma_c	critical Marangoni number based on the height H: $Ma_c = -\frac{\partial\sigma}{\partial T}\frac{\Delta T_c H}{\mu\alpha}$
Ma_c^*	critical Marangoni number based on the geometry factor R^2/H: $Ma_c^* = -\frac{\partial\sigma}{\partial T}\frac{\Delta T_c R^2}{\mu\alpha H}$
Pr	Prandtl number
R	liquid bridge radius [m]
T_C	temperature of the lower (cold) disk [°C]
T_H	temperature of the upper (hot) disk [°C]
v	velocity [m/s]
V	instantaneous liquid bridge volume [m^3]
VR	volume ratio [−]
z	axial coordinate [m]

Greek symbols

α	thermal diffusivity [m^2/s]
Γ	aspect ratio ($= H/R$)
ΔT	temperature difference between the disks, $T_H - T_C$ [K]
ΔT_c	critical temperature difference between the disks [K]
λ	wavelength [m]
μ	dynamic viscosity [$kg\,m^{-1}\,s^{-1}$]
$\partial\sigma/\partial T$	temperature coefficient of surface tension [$N\,m^{-1}\,K^{-1}$]

Several experiments have been conducted in the past yielding data useful for verification of numerical results. Preisser et al. [2] and Velten et al. [4] have experimentally studied certain aspects of transition to oscillatory Marangoni convection for high-temperature melts of KCl ($Pr = 1$) and $NaNO_3$ ($Pr = 7$). They measured the critical temperature difference, ΔT_c, and the frequency of temperature oscillations for a disk diameter of 6 mm and various aspect ratios. Chun and Wuest [6] and Vargas [7] have also reported critical Marangoni-number data for methanol ($Pr = 7$). Some of these experimental data have been used by Wanschura et al. [8] and Leypoldt et al. [9] for comparisons with numerical linear-stability analysis and numerical simulation predictions, respectively.

Wanschura et al. [8] and Leypold et al. [9] showed that for an intermediate Prandtl number of 4, the axisymmetric steady flow becomes linearly unstable to a pair of hydrothermal waves propagating azimuthally, similar to that in plane layers [10]. Since their numerically predicted critical Marangoni numbers and flow structures compared favorably with the experimental data of Velten et al. [4], the instability mechanism for intermediate Prandtl number fluids may be of hydrothermal-wave type. Nienhuser and Kuhlmann [11] further investigated the effects of shape deformation and buoyancy due to gravity numerically. The hydrothermal waves were characterized by internal temperature fluctuations which arise in the region of large (radial) basic-state temperature gradients. The basic temperature field which is crucial for the instability mechanism was found to be susceptible to the buoyant convection transport rather than the hydrostatic deformation of the liquid bridge for $Pr = 4$.

Although Velten et al. [4] pointed out that there may be a significant influence of heat and mass transfer at the free surface, the effect of this heat loss on the stability of Marangoni convection in liquid bridges has not been fully clarified yet. Through a linear-stability analysis, Kuhlmann and Rath [12] pointed out that the enhanced surface heat loss would affect the Marangoni flow in a liquid bridge by reducing the radial temperature gradients and the strength of the surface shear flow so that the disturbances would not be able to extract as much energy from the base state as for the case of no heat loss. Recently, Kamotani et al. [13] have experimentally measured the effect of surface heat loss for higher Prandtl number fluids ($Pr = 24$–49) by varying the surrounding air temperature relative to the hot and cold disk temperatures. The enhanced heat loss from the surface exposed to air clearly resulted in the destabilization of Marangoni flow and significantly lower critical Marangoni numbers were obtained compared to the case of no surface heat loss.

In the present work, Marangoni convection experiments have been conducted using acetone with $Pr = 4.3$, which is a volatile liquid and involves significant heat and mass transfer at the liquid surface due to evaporation. Because of the latent heat involved, the magnitude of heat loss is expected to be much greater than that for convection alone, thus it would be possible to study the effect of free surface heat and mass transfer on the transition from steady to oscillatory Marangoni convection if the evaporation rate can be varied.

Acetone has been used previously in Marangoni convection experiments involving horizontal liquid layers in rectangular cavities by Villers and Platten [14] and by Braunsfurth and Homsy [15]. By placing a plate above the test section, both of those experiments were conducted only under reduced evaporation rates. In the present work, different evaporation rates were realized by placing a partially or tightly sealed enclosure around the liquid bridge. To yield experimental data that would be useful for the understanding of the physical phenomena, different measurement techniques have also been utilized.

2. Experimental apparatus and instrumentation

A schematic of the experimental apparatus is shown in Fig. 1. Two slightly different test sections, A and B, used

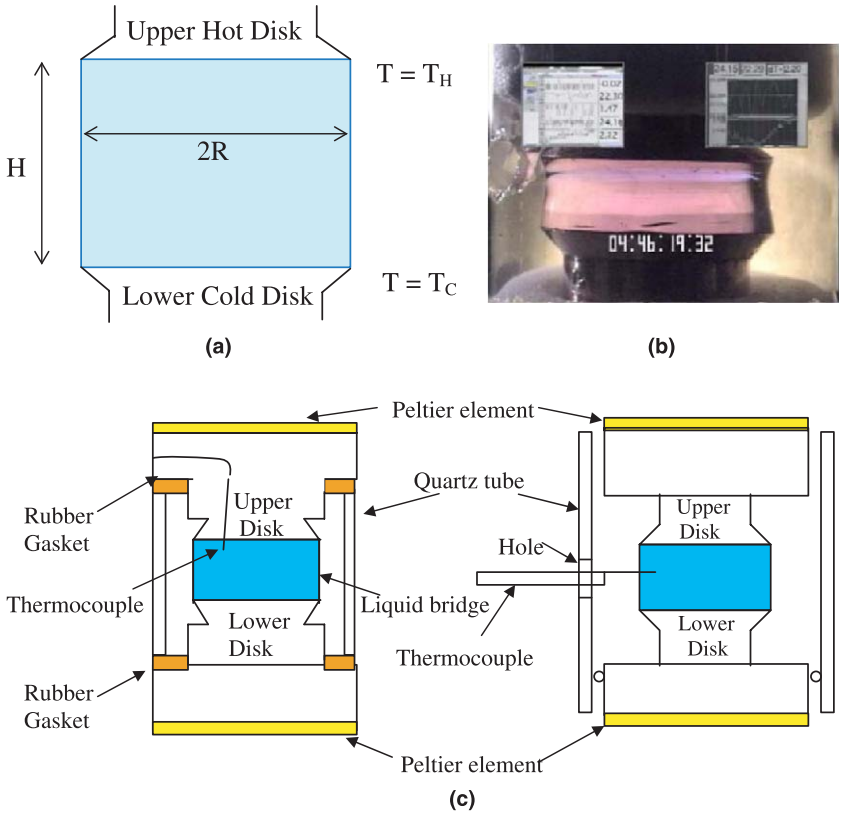

Fig. 1. Experimental apparatus: (a) sketch of the liquid bridge, (b) photograph of the acetone bridge with simultaneous recording and display of image and temperature data, and (c) schematic of the test sections A (reduced evaporation case or partially open case) and B (fully open case).

in the experiments consisted of upper and lower disks between which an acetone liquid bridge could be formed. The upper and lower disks with 5.0, 7.0 or 10.0 mm diameter (D) were made of brass, copper, or sapphire rods as summarized in Table 1, depending on the type of measurement required. The copper and brass disks were tapered at the end as shown in Fig. 1, while sapphire disks were straight rods with flat polished ends. Each disk was attached to a Peltier element connected to a DC power supply as well as a constant temperature circulation bath to be either heated or cooled independently. The lower disk had a small hole drilled through the axis so that acetone could be injected into the gap between the upper and lower disks to form a liquid bridge. A syringe was used to inject the liquid, either manually or using a linear actuator.

Acetone has significantly greater volatility than higher Prandtl number fluids such as silicone oils. In order to reduce the rate of surface evaporation and thinning of the liquid bridge with time, a quartz tube was placed with a gap of 2–3 mm around the liquid bridge in both test sections. The test section A with 7.0 mm diameter disks could be tightly sealed (reduced evaporation case) or partially open (stronger evaporation case).

The test section A was sealed by placing natural rubber gaskets between the brass bases and the top and bottom ends of the quartz tube as shown in Fig. 1(c). Furthermore, a micro-thermocouple used to detect the liquid temperature fluctuations at the onset of oscillatory convection was inserted through a hole in the upper disk to avoid breaking the seal. This test section was used to investigate the reduced evaporation case. For the partially open system with a relatively high evaporation rate, the upper rubber gasket was removed so that a gap existed between the quartz tube and the brass base at the top.

On the other hand, the test section B with 5.0 or 10.0 mm diameter disks, could not be tightly sealed due to its design. Besides, the quartz tubes also had several holes of 2–3 mm diameter drilled to allow insertion of one or two micro-thermocouples into the liquid bridge from the outside to measure the liquid temperature oscillations as shown in Fig. 1(c). Thus, only the strongly evaporating case was investigated for the disk diameters of 5.0 and 10.0 mm. Quartz tubes of different lengths were used in both test sections to allow the liquid bridge height and the aspect ratio to be changed.

Table 1
Disk materials and diameters used

Diameter (mm)	Lower disk/upper disk
5.0	Copper/ZnSe
	Copper/sapphire
7.0	Brass/brass
10.0	Copper/copper
	Copper/ZnSe

The temperature measurement on the liquid bridge surface was also made with the test section A using an infrared imager. A rectangular Pyrex glass enclosure with one face made of a small infrared-transmitting ZnSe plate was placed around the liquid bridge instead of a quartz tube to allow for infrared imaging. These measurements were performed for both closed and partially open systems with disks of $D = 7.0$ mm.

2.1. Disk and fluid temperature measurements

Thermocouples were used to accurately measure the hot and cold disk temperatures, T_H and T_C, disk-temperature difference, ΔT ($= T_H - T_C$), and local liquid temperature. In preliminary experiments with the test section B, the onset of oscillatory Marangoni convection in acetone bridges was found to occur at very small temperature differences, $\Delta T < 2$ K, at which periodic liquid temperature oscillations with amplitudes less than 0.01 K appeared. Thus, the temperature data had to be obtained with precisely calibrated thermocouples (T/C's) and the T/C signals had to be amplified and recorded by a data acquisition system with little noise.

The hot and cold disk temperatures were measured using type-T micro-thermocouples with a wire diameter of 75 μm. Small holes of 0.5 mm diameter and 2–4 mm depth were drilled in the brass or copper disks from the side at 2–3 mm from the disk's end surface. The thermocouple junction was then placed into each hole and anchored there by filling the hole with thin needle-shaped strips of Teflon. The use of any cement such as epoxy was avoided in order to prevent any contamination of the working fluid.

To measure ΔT, a pair of type-T thermocouples attached to the hot and cold disks was connected in series and the cold junctions were enclosed in a thick-walled aluminum box to directly measure the temperature difference. This arrangement made possible a sensitive measurement of ΔT without incurring a large uncertainty.

Liquid temperature oscillations were measured using type-E micro-thermocouples inserted into the liquid bridge. For the test section A, the 75 μm diameter T/C wires were inserted through the upper disk and the T/C junction was positioned well inside the liquid bridge about 1 mm below the upper disk surface. For the test section B, a thermocouple junction of 25 μm diameter wires was inserted into the liquid bridge from the side through a small hole drilled in the quartz-tube wall.

Calibration of all the thermocouples was conducted using a platinum resistance thermometer sensor (Pt-100) with an absolute error of $< \pm 0.03$ K. All the disk and fluid thermocouples were calibrated at 0, 15.0, 20.0 and 25.0 °C, while the thermocouple pairs for ΔT measurement were calibrated at 0, 1.0, 2.0, 3.0, 7.0 and 10.0 °C with T_H kept at 24–25.5 °C. The uncertainty in temperature and ΔT measurements was estimated to be ± 0.05 K.

To sample and record the temperature data, the thermocouple signals had to be amplified and recorded with as little noise as possible. A PC-based National Instruments Data Acquisition System (Model PCI-6035E with SCXI-1102) was used with the test section A, and a Hewlett–Packard Data Acquisition/Control Unit (Model 3852A) and a workstation with the test section B. For the liquid temperature and ΔT measurements, high-gain, low-noise DC amplifiers (NEC Model 6L06H) were used in both test sections to amplify the T/C signals before the data acquisition system to maximize the signal to noise ratio. With the above temperature measurement systems, periodic liquid temperature oscillations of amplitudes as small as 0.01 K could be clearly identified and recorded. All the temperature data were sampled using Labview software at a rate of 10 Hz, stored in files and graphically displayed in real-time alongside the image of the liquid bridge on the video monitor.

2.2. Flow visualization

Tracer particle imaging and photochromic dye activation (PDA) techniques were used to measure the bulk flow pattern and surface velocity, respectively. For the tracer particle imaging technique with a vertical laser light-sheet, silver-coated particles of 8–12 μm diameter and specific gravity of 1.05–1.15 were dispersed in acetone.

In addition, to monitor three-dimensional flow patterns, Fillite™ particles with 32–53 μm diameters were mixed with the liquid and illuminated by a cold light source placed behind the liquid bridge. The Fillite™ particle motion was monitored with a CCD camera situated on the side of the liquid bridge opposite to the light source.

2.3. Surface velocity measurement

The surface velocity was measured using a photochromic dye activation technique, which has been previously used in various gas–liquid flow experiments [16,17]. It uses a UV pulse laser (N_2 gas laser, $\lambda = 337$ nm) to activate the molecules of a photochromic dye called TNSB, dissolved in the working liquid at a concentration of 100–500 ppm. The acetone-dye solution is transparent, but changes to a purple color upon UV irradiation. The purple liquid acts as a tracer and the dye trace motion can be monitored by a color video camera to obtain the liquid surface velocity as shown in Fig. 2.

Although the laser beam penetrated some distance into the liquid, the fastest moving part of the trace from near the top to the bottom of the liquid bridge can be considered to represent the surface velocity, because the velocity of the basic two-dimensional flow decreases monotonically from the surface with the penetration depth of the laser light, as known from numerical calculations. Although the same technique has been used previously to measure the velocity of a liquid layer surface in a rectangular cavity under Marangoni convection [18,19], to our knowledge, this work presents the first direct measurement of the surface velocity oscillations at the onset of oscillatory Marangoni convec-

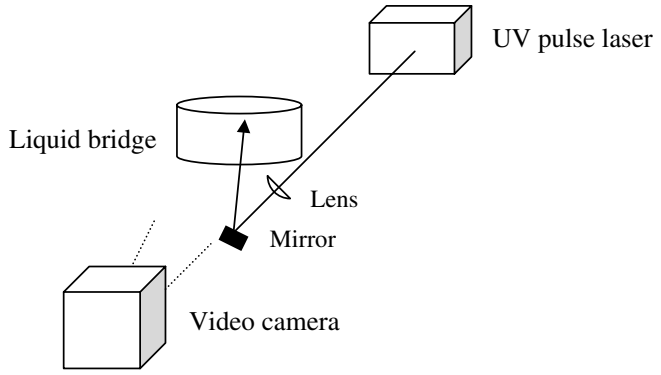

Fig. 2. Photochromic dye activation set-up for surface velocity measurements.

tion in a half-floating zone of intermediate to high Prandtl numbers.

2.4. Surface oscillation measurement

Another measurement attempted was the amplitude of surface oscillation, which has been hypothesized to play an important role in the mechanism governing the onset of oscillatory Marangoni convection in a half-floating zone at high Prandtl numbers [3,20]. Recently, Kitagawa et al. [21] successfully used a Laser Focus Displacement Meter (Keyence Model LT-8100) to measure the surface oscillations in 10 cSt silicone oil liquid bridges. Thus, the same instrument with 0.2 μm resolution was used in the present work.

3. Experimental conditions and procedure

Experiments were performed under different evaporation conditions using either a tightly sealed or partially open quartz tube placed around the liquid bridge. The main parameters varied in the experiments were the aspect ratio, $\Gamma = H/R$, (by varying either H, R, or both), and the volume ratio, VR, as shown in Table 2. The parameter ranges covered and different types of instrumentation used are also shown. While all the disk diameters were used to obtain data for the strongly evaporating case, the reduced evaporation experiments were performed only with the 7.0 mm diameter disks.

For each disk diameter, the liquid bridge height, H, was fixed at a specified value corresponding to a given aspect ratio. In each run, the liquid was injected into the bridge to maximize the initial volume ratio and then the disk-temperature difference, ΔT, was either increased or decreased slowly at rates shown in Table 3 by changing the voltage supplied to the Peltier element attached to the lower (cold) disk, while the upper (hot) disk temperature was kept nearly constant at room temperature (23–25 °C). The disk-temperature difference, ΔT, was varied as slowly as possible at a relatively constant rate to cross the critical temperature difference and achieve transition from steady to oscillatory flow or vice versa before the volume ratio decreased to less than about 0.8–0.9 due to evaporation.

Table 3
Temperature ramping rate to set disk-temperature difference, ΔT

System and disk diameter	$d\Delta T/dt$ (K/s)
Partially open system, $D = 5.0$ mm	0.008
Closed system, $D = 7.0$ mm	0.003
Partially open system, $D = 7.0$ mm	0.005
Partially open system, $D = 10.0$ mm	0.003

3.1. Effects of impurities on acetone properties and surface contamination

The thermophysical properties of acetone are summarized in Table 4. In order to minimize the effect of impurities contained in the working fluid, acetone with 99.5% and 99.9+% purity were tested both with and without zeolite treatment to reduce the residual water content. The preliminary tests, however, indicated no significant effects of purity and residual water content on the critical ΔT values. Thus, in the present work, acetone with 99.9+% purity from Aldrich without any zeolite treatment was used in all the experiments. The temperature-dependent surface tension coefficient was measured with and without a photochromic dye (500 ppm concentration) and tracer particles. The surface tension measurements at different temperatures using a plate pulling method with Kyowa surface-tensiometer (Model CBVP-Z) yielded no significant differences

Table 4
Thermophysical properties of acetone

T (°C)	μ (mPa s)	C_p (kJ/kg °C)	K (W/m °C)	Pr
0	0.398	2.102	0.165	5.1
20	0.325	2.156	0.160	4.4
27	0.301	2.214	0.159	4.2
47	0.250	2.265	0.152	3.7

Note: At 23 °C, $\sigma = 23.4$ mN/m, $\gamma = -0.1262$ mN/m/K, $\rho = 787$ kg/m^3.

Table 2
Experimental conditions

Diameter, D (mm)	Height, H (mm)	Aspect ratio ($\Gamma = H/R$)	Volume ratio, VR	Instrumentation used
5.0	1.5–4.0	0.6–1.6	0.81–1.05	PD, TPI
7.0	2.0–4.5	0.55–1.28	0.7–1.1	PD, TPI, IR-S
10.0	1.5–4.0	0.3–0.8	0.84–1.06	PD, TPI, LFDM

PD: Photochromic dye activation method for surface velocity measurement, TPI: tracer particle imaging for flow pattern observation, IR-S: infrared imager for surface temperature distribution measurement, LFDM: laser focus displacement meter.

(<2%) between 99.9+% pure acetone and the working solutions.

Although the liquid bridge was surrounded by a quartz tube and not directly exposed to the ambient air, fresh liquid was injected to overflow from the lower disk and renew the liquid bridge surface at the beginning of each measurement in order to avoid collection of data with a contaminated liquid bridge surface.

4. Results and discussion

4.1. Acetone bridge shape and evaporation rate

The shape of the liquid bridge and the instantaneous volume ratio could be readily obtained from the video images using an image analysis program on a PC. The interface shape was first digitized and the disk radius, R, was used for calibration of the scale. The local radius of the liquid bridge was then calculated from the free surface coordinates at different heights above the lower disk. The instantaneous liquid bridge volume, V, was calculated by numerically integrating the local radius–height data, and the volume ratio was obtained as $\mathrm{VR} = V/\pi R^2 H$. By measuring the volume ratios at the beginning ($\mathrm{VR} > 1.0$) and after a sufficient amount of time elapsed, the average evaporation rate could be quantified as the volume reduction rate expressed as volume % per second (vol.%/s). As shown in Table 5, the evaporation rate for the partially open case decreased strongly with the liquid bridge diameter for the test section B ($D = 5.0$ and 10.0 mm). This is reasonable since the exposed surface area increases linearly with the diameter, but the liquid bridge volume increases as the square of the diameter. The evaporation rate data for $D = 7.0$ mm and different aspect ratios are shown for both the closed and partially open systems in Fig. 3. In both systems, the evaporation rate decreased with the increasing aspect ratio. At all the aspect ratios tested, the partially open system showed about 4–5 times higher evaporation rates than those for the closed system. Also shown in Fig. 3 is the fully open system for $\Gamma = 1.1$, which indicates that fully exposing the acetone bridge to the ambient air increases the evaporation rate by about 7 times when compared to the closed system.

As is clear from the above, even the tightly sealed case showed the effect of surface evaporation and the liquid bridge gradually became thinner with time, although the rate of evaporation was significantly reduced compared to the partially and fully open cases. Mass transfer from the bridge surface continued to occur even in the closed system because the system was not entirely isothermal and temperature differences existed between the liquid bridge and the rest of the solid surfaces (the disks and the quartz tube).

Table 5
Volume reduction rate

Diameter (mm)	Volume reduction rate (vol.%/s)
5.0 (Partially open)	0.12–0.19
7.0 (Closed)	0.02–0.10
7.0 (Partially open)	0.13–0.31
10.0 (Partially open)	0.03–0.06

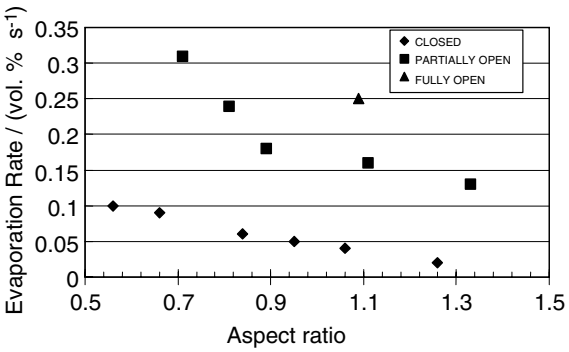

Fig. 3. Evaporation rates in volume percent per second for acetone bridge, $D = 7.0$ mm.

4.2. Effects of evaporation on the surface temperature distribution

The surface temperature distributions measured by an infrared imager under steady flow conditions showed significant differences between the closed and partially open systems, as a result of different rates of evaporative cooling. At reduced evaporation rates in a closed system, variations in the surface temperature distribution were small as shown in Fig. 4(a). As the evaporation rate increased by a factor of 4–5 in the partially open system, the surface was cooled to such an extent that a part of the surface became even cooler than the lower cold disk. This can be observed in Fig. 4(b) as a cold band just above the lower disk, and in a temperature profile along the centerline as shown in Fig. 4(c). The latter figure shows the surface temperature variation relative to the coldest spot on the surface. The error bars indicate the width of the color scale and the region of uniform temperature indicated by a given color band in the infrared image.

The evaporative cooling effect intensified further when the quartz tube was removed from the test section and the acetone bridge was fully exposed to the ambient air as shown in Fig. 4(d) and (e). Thus, in both the partially and fully open systems, an inversion in the temperature gradient occurred near the cold disk.

4.3. Determination of ΔT_c at the onset of oscillatory Marangoni convection

In the experiment, the disk-temperature difference, ΔT, was varied to either increase or decrease past the critical temperature difference corresponding to the transition from steady to oscillatory Marangoni convection while

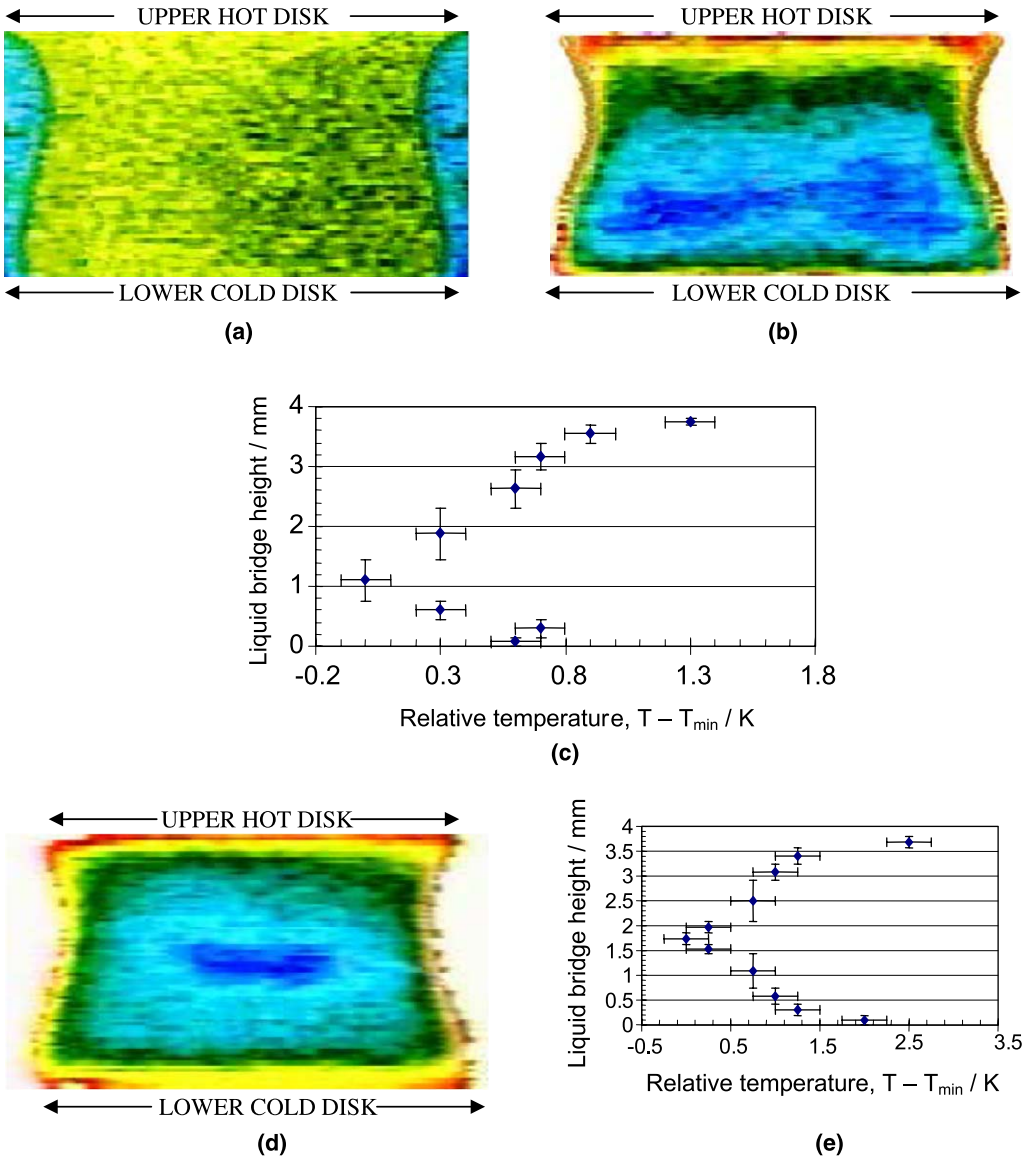

Fig. 4. Surface temperature distributions for $D = 7.0$ mm, $\Gamma = 1.1$, VR $= 0.9$ and liquid bridges of different evaporation rates (ER): (a) IR image for a closed system (ER ≈ 0.035 vol.%/s), (b) IR image for a partially open system (ER ≈ 0.16 vol.%/s), and (c) temperature profile along the centerline for the partially open system, (d) IR image for a fully open system (ER ≈ 0.25 vol.%/s), and (e) temperature profile along the centerline for the fully open system.

the volume ratio of the liquid bridge was allowed to slowly decrease due to evaporation. For each disk diameter and aspect ratio, fluid and disk temperature measurements were made several times to check the reproducibility of the critical ΔT data.

At or slightly above ΔT_c corresponding to the onset of oscillatory convection, the following phenomena were observed to occur for both the closed and partially open systems:

1. Harmonic fluid-temperature oscillations.
2. Surface-velocity fluctuations with an appearance of an azimuthal component.
3. Vortex expansion and contraction in tracer particle images at a constant azimuthal position.
4. Harmonic thermal waves on the free surface.

When the disk-temperature difference was gradually reduced from above to below ΔT_c, these phenomena disappeared and a steady flow returned, however, the oscillatory flow characteristics persisted until ΔT fell clearly below ΔT_c found for the onset. Each of the above phenomena observed is discussed in detail below.

4.3.1. Fluid-temperature oscillations

The fluid temperature measured at the onset of oscillatory convection by a micro-thermocouple started to show a periodic oscillation with an amplitude increasing from less than 0.01 K to greater than 0.1 K, at a certain frequency between 0.5 and 1 Hz, which depended on the aspect ratio. For example, the oscillation frequency of the liquid temperature was 1.0 Hz when the liquid bridge aspect ratio was $\Gamma = 0.6$, and 0.5 Hz when the aspect ratio

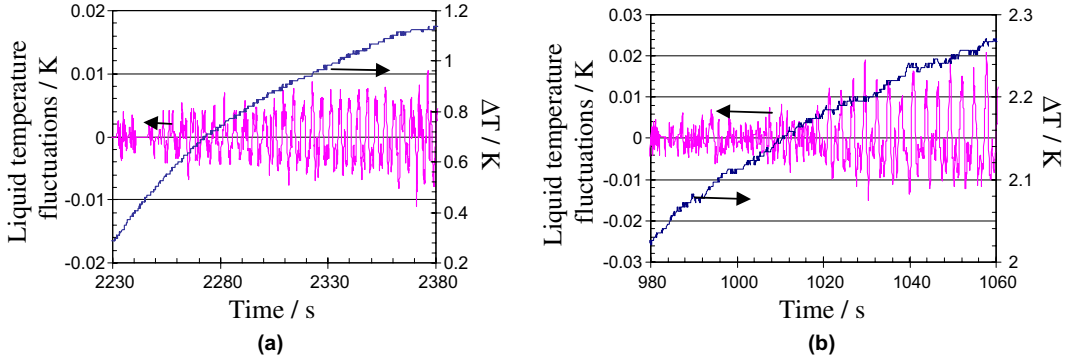

Fig. 5. Liquid temperature oscillations at the onset of oscillatory convection ($D = 7.0$ mm, $\Gamma = 1.1$): (a) closed system and (b) partially open system.

was $\Gamma = 1.3$. Sample data for $D = 7.0$ mm and $\Gamma = 1.1$, are shown in Fig. 5(a) and (b) for the closed and partially open systems, respectively. Both data indicate a gradual increase in the liquid temperature oscillation amplitude well beyond the noise level at the onset of oscillatory flow, once ΔT is increased above a critical value, ΔT_c.

4.3.2. Surface-velocity fluctuations

For the closed system, the photochromic dye traces formed near the upper disk in steady flow at $\Delta T < \Delta T_c$, always traveled vertically down to the same azimuthal position near the lower disk indicating an axisymmetric flow. Because the dye traces always traveled along the closed streamlines many times before they decayed in color and disappeared, the successive traces appeared as a thin vertical band as shown in Fig. 6(a). But at the onset of oscillatory flow, the dye trace trajectory started to oscillate in the azimuthal direction, towards both the left and right of the vertical trajectory as shown in Fig. 6(b). Note that a hole used for acetone injection is seen in the lower disk in Fig. 6.

The change in the surface velocity from a purely one-dimensional (downward) trajectory to a two-dimensional trajectory with a continuously changing azimuthal component was observed to occur nearly simultaneously with the appearance of the liquid temperature oscillations described previously. The maximum inclination angle of the trace trajectory was found to be about 30° from the vertical for the closed system with $D = 7.0$ mm, and at $\Delta T = 0.85$ K, well above the ΔT_c of 0.5 K. Thus, the maximum azimuthal-to-vertical velocity ratio for this case would be equal to tan 30° or 0.58.

The photochromic dye activation technique showed different surface velocities in the partially open and closed systems. In the partially open system, even in steady flow, the dye traces traveled at a certain angle with respect to the vertical (Fig. 6(c)). At the onset of oscillatory convection, the dye trace started fluctuating in the azimuthal direction from the steady, inclined trajectory. Fig. 6(d) shows the dye trace trajectories at $\Delta T = 2.27$ K, which is above the critical value ($\Delta T_c \approx 1.7$ K). Besides the dye traces showing oscillating azimuthal displacements, the Fillite™ particles also changed their motion from a purely up–down motion to the flow with an azimuthal component, during which individual particles were tracing a figure of infinity (∞) as viewed by the video camera. Furthermore, at sufficiently large values of $\Delta T \gg \Delta T_c$, the amplitude of the vertical motion of the Fillite™ particles at a given azimuthal position visibly oscillated in time. At a given instant of time, the amplitude of this oscillation showed a sinusoidal modulation in the azimuthal direction which could be detected by observations from the side of the liquid bridge. Hence, the tracer-particle motion reflected an azimuthally traveling wave.

From the photochromic dye trace images obtained for $D = 7.0$ mm and $\Gamma = 1.1$, the downward surface velocities were obtained for the closed system with reduced evaporation rates for which $\Delta T_c = \sim 0.5$ K. Fig. 6(e) shows the axial component of the average surface velocity between the hot and cold disks over nearly the entire liquid bridge height. The average surface velocity increases almost linearly with an increase in ΔT from a steady to oscillatory flow ($\Delta T_c = \sim 0.5$ K).

4.3.3. Vortex expansion and contraction

In the tracer particle images of the flow patterns in the vertical cross section, a pair of vortices appeared near the liquid bridge surface representing a toroidal vortex. The pair of vortices had the same size constant in time during steady flow, indicating an axisymmetric flow with the vertical return flow upward along the axis of the liquid bridge. At the onset of oscillatory flow, however, the vortex started to expand and contract on opposite sides as shown in Fig. 7 at the same frequency as the temperature oscillations, as previously reported by Chun and Wuest [6], among others. The flow then became non-axisymmetric and the return flow was no longer vertical along the axis of the liquid bridge.

4.3.4. Surface temperature variation

For the closed system with reduced evaporation rates, the surface temperature recorded by an infrared imager showed the propagation of a thermal wave in the azimuthal direction shortly after the onset of oscillatory flow. Alternating cold and hot patches moved from right to left in

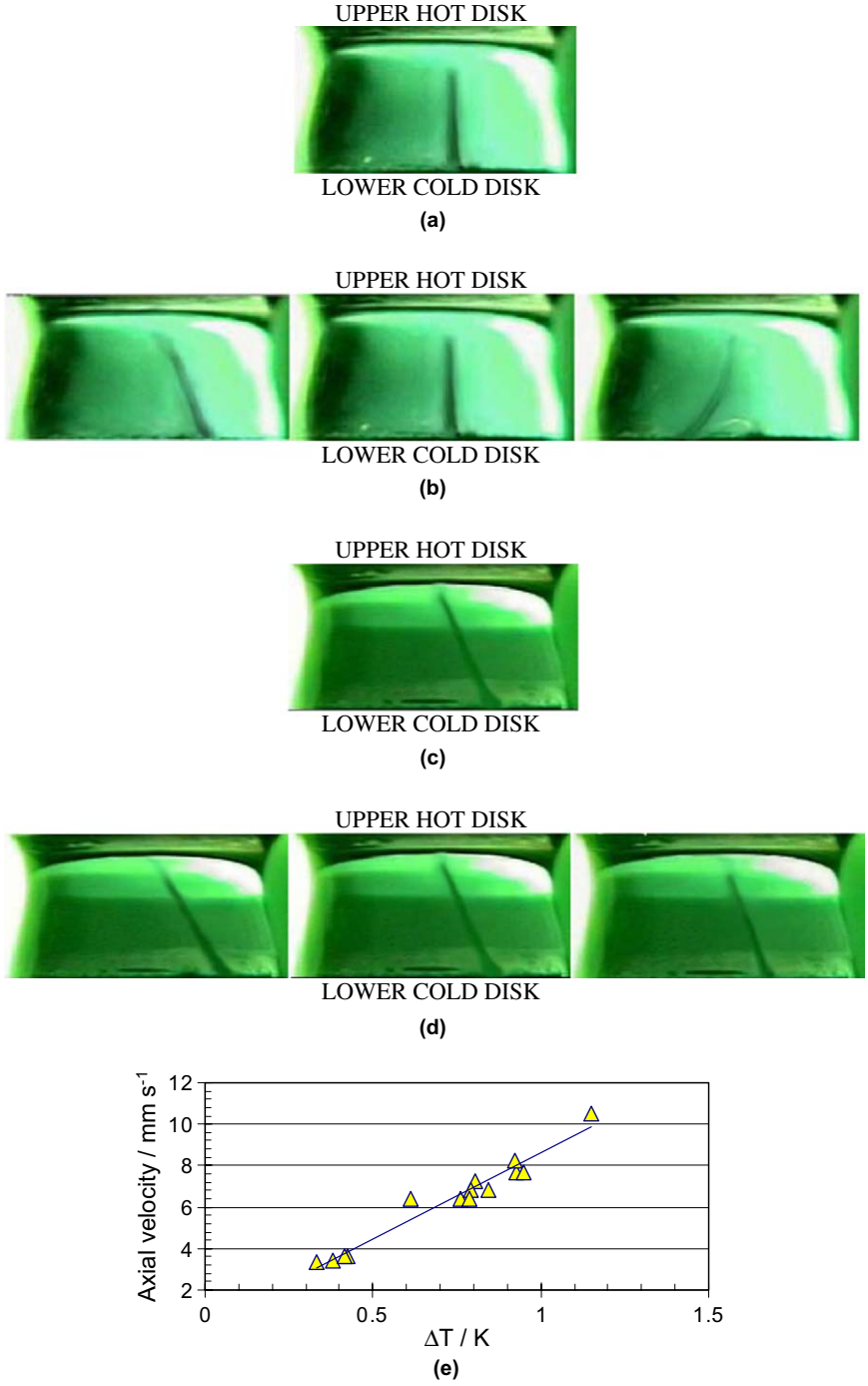

Fig. 6. Trajectory of photochromic dye traces on the liquid bridge ($D = 7.0$ mm, $\Gamma = 1.1$, VR $= 0.9$): (a) steady flow in a closed system, (b) oscillatory flow in a closed system taken at intervals $\Delta t = 1.1$ s or 1/4 of a period, when $\Delta T = 0.85$ K and $\Delta T_c = 0.5$ K, (c) steady flow in a partially open system, (d) oscillatory flow in a partially open system when $\Delta T = 2.27$ K and $\Delta T_c = 1.7$ K, and (e) surface velocity dependence on ΔT in the closed system.

the side view (clockwise direction) at the same frequency as the liquid temperature oscillations detected in the bulk by a micro-thermocouple. The direction of thermal wave propagation was observed more often in the counter-clockwise direction than in the clockwise direction as viewed from the top of the liquid bridge. Although the direction was seen to sometimes change from the counter-clockwise to the clockwise direction, this change in the direction of wave propagation was not periodic and also infrequent.

In the partially open system with enhanced evaporation rates, temperature distributions during the steady flow showed the existence of a cold region just above the lower (cold) disk. This cold region had a lower temperature than the lower disk. At the onset of oscillatory flow, the cold region started to fluctuate in z-direction (height) with the same frequency as the liquid temperature fluctuations. The fluctuation of the cold region was accompanied by the propagation of hydrothermal waves. The width of

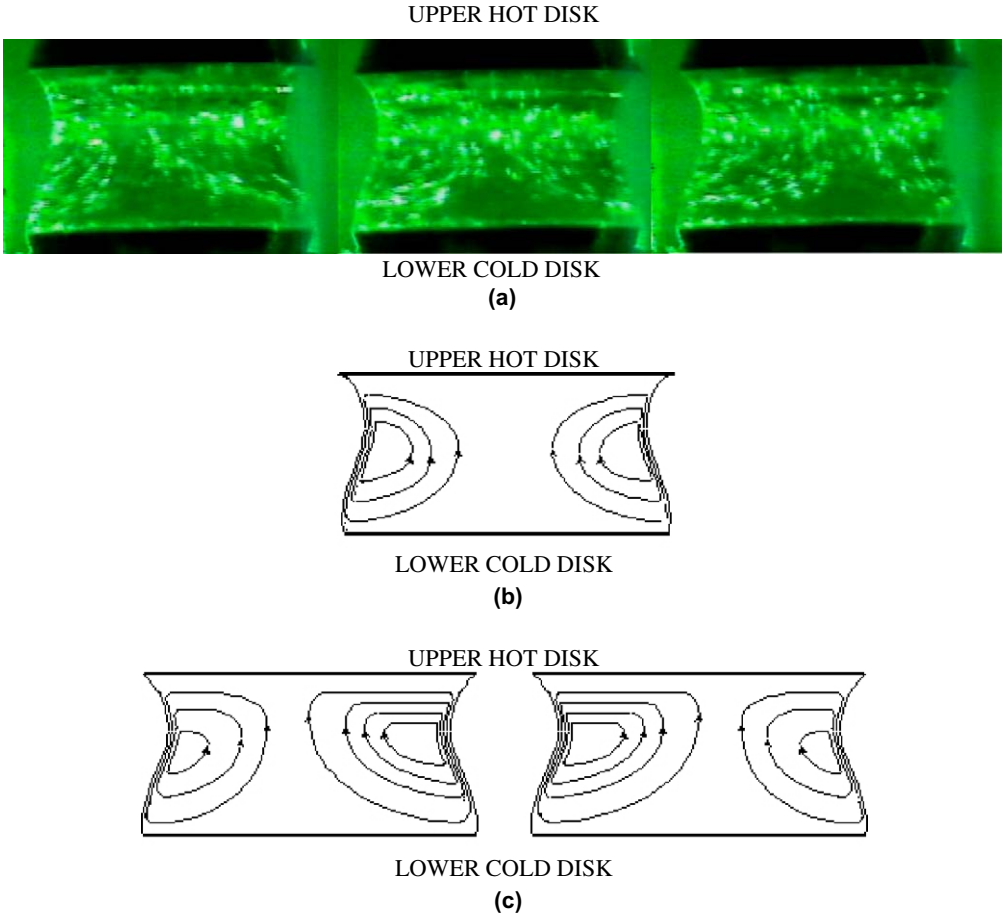

Fig. 7. Toroidal vortex inside a liquid bridge for a volume ratio of 0.9: (a) tracer particle images of oscillatory flow, (b) sketches of the streamlines in steady flow, and (c) sketches of the streamlines in oscillatory flow.

the cold band was modulated in the azimuthal direction and the top edge of this cold band became wavy, again indicating a hydrothermal wave traveling in the azimuthal direction.

For the strongly evaporating case, the azimuthal wave number or mode data could be obtained from the IR images but only at large values of ΔT well above ΔT_c because of the limited sensitivity of the IR imager (0.1 K) and the generally very small amplitudes of fluid-temperature oscillations. The instability modes obtained for $D = 7.0$ mm and different aspect ratios are summarized in Table 6. The modes obtained were generally higher than those given by the relation "mode · aspect ratio = 2.2"

Table 6
Azimuthal wave numbers for acetone in the partially open system ($D = 7.0$ mm)

H (mm)	(H/R)	ΔT (K)	Mode	Mode · aspect ratio
1.5	0.6	4.0	4	2.4
1.5	0.6	4.5	4	2.4
2.0	0.8	3.2	4	3.2
2.5	1.0	2.9	3	3.0
2.5	1.0	3.9	3	3.0
3.25	1.3	3.4	2	2.6

[2]. A better agreement is expected at smaller values of ΔT close to ΔT_c, since the mode numbers have been reported to increase with ΔT [4].

4.3.5. Surface oscillations

Surface oscillation measurements could be made only for the partially open system, by passing a laser beam from the Laser Focus Displacement Meter through a hole in the quartz-tube wall. The surface oscillations, however, could not be detected slightly after the onset of oscillatory flow for $D = 5.0$ and 10.0 mm. Even for $\Delta T \gg \Delta T_c$ the surface oscillation could barely be detected. We, therefore, conclude that the surface oscillations must have been less than the minimum sensor resolution of 0.2 μm, if they occurred at all.

4.4. Critical temperature difference and Marangoni number at the onset of oscillatory convection

Liquid temperature oscillations detected by a microthermocouple inserted into the liquid bridge were examined to determine the critical temperature difference, ΔT_c, at the onset of oscillatory flow for various disk diameters and aspect ratios. The analysis was performed by first taking

moving averages of the instantaneous temperature data to obtain the mean liquid temperature, and then subtracting the mean temperature from the instantaneous temperature to obtain the fluctuating component as a function of time. The liquid temperature oscillations were then plotted against time together with the temperature difference between the hot and cold disks, as shown earlier in Fig. 5(a) and (b) for the closed and partially open systems, respectively. In both cases, before the onset of oscillatory flow, the liquid temperature data showed random fluctuations with a small amplitude of about ±0.01 K, considered to be the background noise. At the onset of oscillatory flow, periodic liquid temperature oscillations appeared with a certain frequency and started to grow larger in amplitude.

When the disk-temperature difference was reduced from above ΔT_c, the periodic temperature oscillations gradually decreased in amplitude and disappeared at a certain ΔT slightly below ΔT_c. This was common to both closed and partially open systems, and is attributed to a finite amount of time necessary for the oscillatory motion to fully decay and the flow to reach a stable state.

The present analyses of ΔT_c data for $D = 7.0$ mm and different aspect ratios showed ΔT_c to range from ~0.5 K to 1.1 K in the closed system and 1.8 K to 2.6 K for the partially open system (Fig. 8(a)). The data are shown for both increasing ΔT (square symbols correspond to the ramping up case or steady-to-oscillatory transition) and decreasing ΔT (triangles for the ramping down case or oscillatory-to-steady transition). The critical ΔT data for the ramping up case were always greater than those for the ramping down case, as previously reported by Velten et al. [4]. Significant differences in the critical ΔT values between the closed and partially open systems even for the same disk diameter and aspect ratio are clearly the result of surface evaporation. The partially open system with a higher rate of surface evaporation became more stable and the onset of oscillatory Marangoni convection was delayed until much higher values of ΔT_c were reached compared to the closed system.

In all cases, a strong dependence of ΔT_c on the aspect ratio was found as expected. For the closed system with a disk diameter of 7.0 mm, the value of ΔT_c decreased by more than 50% as the aspect ratio increased from 0.56 to 1. It then increased slightly for $\Gamma > 1$ so that the minimum ΔT_c of about 0.5 K was reached at $\Gamma \approx 1$. The variation in ΔT_c with the aspect ratio was similar for the partially open system. The critical temperature difference (ΔT_c) did not show an appreciable change with the volume ratio, unlike for high Prandtl number fluids [22,23]. In the present experiments, no differences in the values of ΔT_c and critical Marangoni number were observed for a given liquid bridge for different volume ratios between 0.7 and 1.1.

The critical Marangoni number, Ma_c, was next calculated based on the measured values of ΔT_c and the liquid bridge height, H. The critical Marangoni-number data

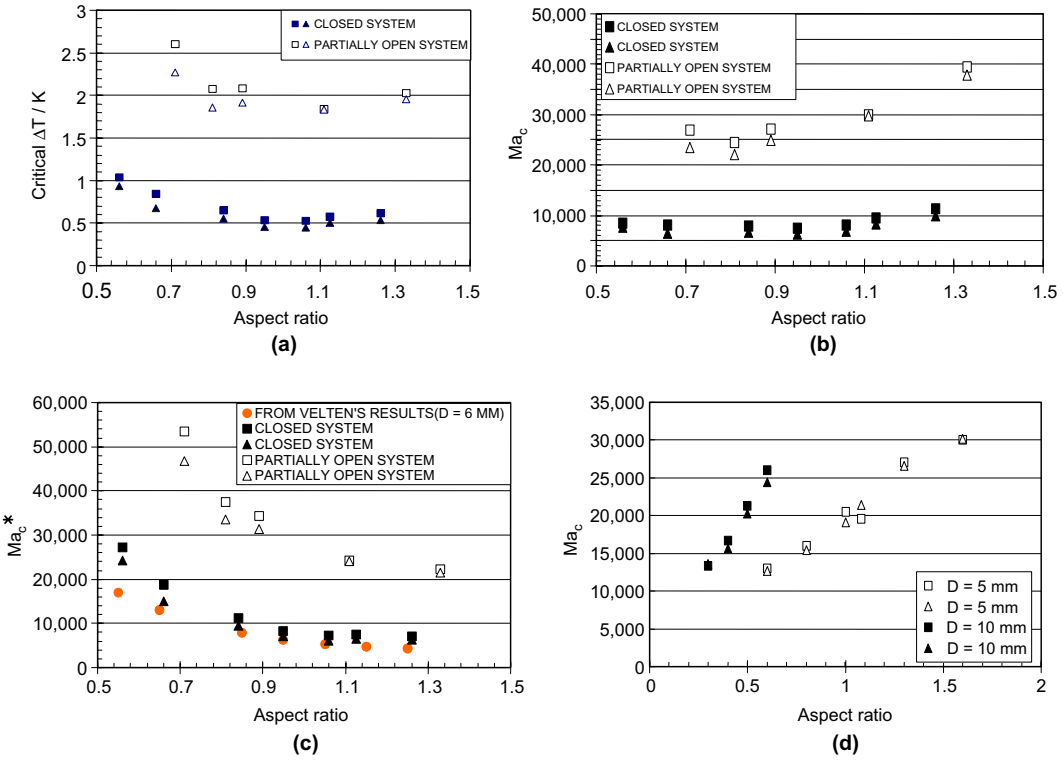

Fig. 8. Onset of oscillatory Marangoni convection data for closed and partially open systems with $D = 7.0$ mm: (a) critical temperature difference data, (b) variation of critical Marangoni number, Ma_c, with aspect ratio Γ, (c) variation of Ma_c^* with aspect ratio Γ, and (d) variation of Ma_c with aspect ratio Γ for $D = 5.0$ and 10.0 mm in a partially open system (square symbols for ramping up and triangles for ramping down).

for a volume ratio of about 0.9–1.0 are plotted against the aspect ratio in Fig. 8(b) for $D = 7.0$ mm and both closed and partially open systems. Velten et al. [4] used a different definition of the Marangoni number, $Ma_c^* = Ma_c/\Gamma^2$, so the present data are also plotted in Fig. 8(c) together with the critical Marangoni numbers interpolated for $Pr = 4.3$ from Velten et al.'s [4] data for $Pr = 1$ and 6.9 obtained for a disk diameter of 6.0 mm. The critical Marangoni numbers, Ma_c^*, for the closed system are seen to be consistent with the values interpolated from Velten et al.'s [4] data. For the closed system with reduced evaporation rates, the critical Marangoni number Ma_c^* decreased strongly with the aspect ratio, while Ma_c was nearly constant for $\Gamma < 1$ and increased slightly for $\Gamma > 1$.

In Fig. 8(d), the critical Marangoni number data are shown for different disk diameters of 5.0 and 10.0 mm in a partially open system only. The critical Marangoni number is seen to increase with the aspect ratio for both diameters in the ranges of the aspect ratios investigated.

4.5. Stabilizing effect of evaporation

The present ΔT_c and critical Marangoni-number data for the closed and partially open systems clearly indicate that heat and mass transfer at the free surface of a liquid bridge due to evaporation significantly stabilizes Marangoni convection in a liquid bridge. This is opposite to the destabilization effect observed by Kamotani et al. [13] and predicted by Kuhlmann and Rath [12] for high Prandtl number fluids.

From the evaporation rate data shown in Fig. 3 and the latent heat of vaporization ($h_{fg} = 524$ kJ/kg at 20 °C) for acetone, it is possible to calculate the rate of surface heat loss, Q, and the Biot number ($Bi = Q/(2\pi Hk\Delta T_{L-A})$) assuming the difference between the average liquid bridge temperature and the surrounding air temperature, ΔT_{L-A}, to be 2 °C. For an aspect ratio of ~1, the evaporation rates were 0.04 and 0.16 vol.%/s for the closed and partially open systems, respectively. Using the exposed surface area and latent heat of vaporization, the surface heat loss rates are calculated to be 0.0237 W and 0.095 W, and the Biot numbers are calculated to be 3.2 and 12.7 for the closed and partially open systems, respectively. The Biot number of 3.2 for the closed system is more than twice larger than the maximum Biot number of 1.4 used by Kamotani et al. [13], but the value for the partially open system is an order of magnitude greater. This means that the cooling effect due to evaporation is much greater than that possible with only convective cooling on the free surface.

Such high rates of evaporative cooling of the liquid bridge surface should cause a reduced radial temperature gradient in the bulk liquid which plays an important role in the instability mechanism for intermediate Prandtl number ($0.5 < Pr < 5$) fluids according to the predictions of previous linear-stability analyses [8,11]. Although slight enhancement in surface cooling is destabilizing, significantly enhanced cooling by evaporation can stabilize Marangoni convection and increase the critical Marangoni number by reducing the radial temperature gradients in the liquid bridge, thus reducing the energy necessary for the instability to arise and grow in the liquid bridge. A more quantitative analysis of the evaporation effect on Marangoni convection in liquid bridges of intermediate Prandtl numbers would require a linear-stability analysis that includes the effect of heat loss due to surface evaporation.

5. Conclusions

The effects of liquid evaporation from the free surface on the transition from steady to oscillatory Marangoni convection have been investigated experimentally in acetone liquid bridges with diameters of 5.0, 7.0, and 10.0 mm, and heights of <5 mm. The evaporation rate was varied by partially or completely enclosing the liquid bridge with a quartz tube.

The critical temperature difference (or critical Marangoni number) at which the flow becomes oscillatory, was found to depend strongly on the evaporation rate. The critical temperature difference varied with the aspect ratio (height/radius) ranging from 0.5 to 1.05 K for the closed system with $D = 7.0$ mm, and from 1.6 to 2.6 K for the partially open systems (strongly evaporating case) with $D = 5.0$, 7.0, and 10.0 mm. The present critical Marangoni-number data for $D = 7.0$ mm in a closed system were found to be consistent with the values for $Pr = 4.3$ interpolated from Velten et al.'s [4] data for $D = 6.0$ mm and $Pr = 1$ and 6.9.

The liquid evaporation was found to have a strong stabilizing effect on Marangoni convection, since the critical temperature difference and the critical Marangoni number both increased significantly with the enhanced evaporation rate. This effect was attributable to a significant reduction in the radial temperature gradients due to the enhanced heat loss from the surface in accordance with the predictions of previous linear-stability analyses of Wanschura et al. [8] and Nienhuser and Kuhlmann [11]. As the radial temperature gradient was predicted to play an important role in the instability mechanism for intermediate Prandtl number ($0.5 < Pr < 5$) fluids, the suppression of the radial temperature gradient due to evaporative cooling is thus believed to result in the reduction of the energy necessary for an instability to arise and grow in the liquid.

Acknowledgements

This work was supported by Japan Aerospace Exploration Agency (JAXA) in the framework of the Marangoni Convection Modeling Research project. S. Simic-Stefani was also financially supported by the Canadian Space Agency. The authors would also like to thank Prof. H. Kuhlmann of Vienna University of Technology in Austria for useful discussions.

References

[1] Ch.-H. Chun, W. Wuest, A micro-gravity simulation of the Marangoni convection, Acta Astronaut. 5 (1978) 681–686.

[2] F. Preisser, D. Schwabe, A. Scharmann, Steady and oscillatory thermocapillary convection in liquid columns with free cylindrical surface, J. Fluid Mech. 126 (1983) 545–567.

[3] Y. Kamotani, S. Ostrach, M. Vargas, Oscillatory thermocapillary convection in a simulated float-zone configuration, J. Cryst. Growth 66 (1984) 83–90.

[4] R. Velten, D. Schwabe, A. Scharmann, The periodic instability of thermocapillary convection in cylindrical liquid bridges, Phys. Fluids A 3 (2) (1991) 267–279.

[5] M.F. Schatz, G.P. Neitzel, Experiments on thermocapillary instabilities, Annu. Rev. Fluid Mech. 33 (2001) 93–129.

[6] Ch.-H. Chun, W. Wuest, Experiments on the transition from the steady to the oscillatory Marangoni-convection of a floating zone under reduced gravity effect, Acta Astronaut. 6 (1979) 1073–1082.

[7] M. Vargas, Oscillatory thermocapillary flow in a simulated floating-zone configuration, M.Sc. Thesis, Case Western Reserve University, 1982.

[8] M. Wanschura, V.M. Shevtsova, H.C. Kuhlmann, H.J. Rath, Convective instability mechanisms in thermocapillary liquid bridges, Phys. Fluids 7 (5) (1995) 912–925.

[9] J. Leypoldt, H.C. Kuhlmann, H.J. Rath, Three-dimensional numerical simulation of thermocapillary flows in cylindrical liquid bridges, J. Fluid Mech. 414 (2000) 285–314.

[10] M.K. Smith, S.H. Davis, Instabilities of dynamic thermocapillary liquid layers. Part 1. Convective instabilities, J. Fluid Mech. 132 (1983) 119–144.

[11] C.H. Nienhuser, H.C. Kuhlmann, Stability of thermocapillary flows in non-cylindrical liquid bridges, J. Fluid Mech. 458 (2002) 35–73.

[12] H.C. Kuhlmann, H.J. Rath, Hydrodynamic instabilities in cylindrical thermocapillary liquid bridges, J. Fluid Mech. 247 (1993) 247–274.

[13] Y. Kamotani, L. Wang, S. Hatta, A. Wang, S. Yoda, Free surface heat loss effect on oscillatory thermocapillary flow in liquid bridges of high Prandtl number fluids, Int. J. Heat Mass Transfer 46 (2003) 3211–3220.

[14] D. Villers, J.K. Platten, Coupled buoyancy and Marangoni convection in acetone: experiments and comparison with numerical simulations, J. Fluid Mech. 234 (1992) 487–510.

[15] M.G. Braunsfurth, G.M. Homsy, Combined thermocapillary-buoyancy convection in a cavity: II. An experimental study, Phys. Fluids 9 (1997) 1277–1286.

[16] M. Kawaji, W. Ahmad, J.M. DeJesus, B. Sutharshan, C. Lorencez, M. Ojha, Flow visualization of two-phase flows using photochromic dye activation method, Nucl. Eng. Des. 141 (1993) 343–355.

[17] M. Kawaji, Two-phase flow measurements using a photochromic dye activation technique, Nucl. Eng. Des. 184 (1998) 379–392.

[18] E.T. Tudose, M. Kawaji, An experimental study of thermocapillary convection in a thin horizontal liquid layer in a rectangular cavity under normal gravity with and without controlled vibration, IAF-99-J.4.08, A paper presented at the 50th International Astronautical Congress, October 4–8, Amsterdam, The Netherlands, 1999.

[19] E.T. Tudose, M. Kawaji, An experimental investigation of the onset of oscillations in thermocapillary-buoyant flows in a rectangular cavity, Paper No. NHTC2000-12199, in: Proceedings of the 34th National Heat Transfer Conference, August 20–22, Pittsburgh, Pennsylvania, 2000.

[20] Y. Kamotani, S. Ostrach, Theoretical analysis of thermocapillary flow in cylindrical columns of high Prandtl number fluids, ASME J. Heat Transfer 120 (1998) 758–764.

[21] T. Kitagawa, K. Nishino, S. Yoda, Temperature oscillation and dynamic surface deformation for the onset of oscillatory flow in a liquid column, J. Jpn. Soc. Microgravity Appl. 16 (Supplement) (1999) 100–101.

[22] L.B.S. Sumner, G.P. Neitzel, J.-P. Fontaine, P. Dell'Aversana, Oscillatory thermocapillary convection in liquid bridges with highly deformed free surfaces: experiments and energy-stability analysis, Phys. Fluids 13 (1) (2001) 107–120.

[23] R. Monti, D. Castagnolo, P. Dell' Aversana, G. Desiderio, S. Moreno, G. Evangelista, An experimental and numerical analysis of thermocapillary flow of silicone oils in a micro-floating zone, in: Proceedings of the 43rd Congress of the International Astronautical Federation, Washington, DC, 1992.